PROCEEDINGS OF SPIE

SPIEDigitalLibrary.org/conference-proceedings-of-spie

Geometry and material optimization of long wave infrared Seebeck nanoantennas

González, Francisco, Peale, Robert, Vivas Gomez, Jennyfer, Phelps, Justin, Abdolvand, Reza

Francisco J. González, Robert E. Peale, Jennyfer Vivas Gomez, Justin Phelps, Reza Abdolvand, "Geometry and material optimization of long wave infrared Seebeck nanoantennas," Proc. SPIE 11723, Image Sensing Technologies: Materials, Devices, Systems, and Applications VIII, 117230A (12 April 2021); doi: 10.1117/12.2591299

SPIE.

Event: SPIE Defense + Commercial Sensing, 2021, Online Only

Geometry and material optimization of long wave infrared Seebeck nanoantennas

Francisco J. González[*a,b,c] , Robert E. Peale[a,b], Jennyfer Vivas Gomez[d], Justin Phelps[d], Reza Abdolvand[d]

[a] Physics, University of Central Florida, Orlando, FL USA 32816; [b]Truventic LLC, 1209 W. Gore St., Orlando, FL USA 32805; [c]UASLP; Sierra Leona 550, San Luis Potosi, SLP, Mexico, 78210, [d]Electrical and Computer Engineering, University of Central Florida, Orlando, FL USA 32816

ABSTRACT

Long wave infrared imaging systems require small, low cost and low power systems operating at room-temperature. Seebeck nanoantennas are room temperature detectors which generate voltage due to incident electromagnetic radiation, they also provide polarization sensitivity, directivity, small footprint, tunability and the possibility of integration into electronic and photonic circuits. In this work different materials and fabrication processes used in Seebeck bowtie nanoantennas are numerically simulated in order to optimize its response in the long wave infrared region of the electromagnetic spectrum (8–14 μm.) Gold bowtie nanoantennas with thermoelectric connections made of Bi_3Te_2 and Sb_3Te_2 showed the highest responsivity values of 9 V/W for gold bowtie nanoantennas on a SiO_2 substrate and 240 V/W for gold bowtie free-standing structures. Computer simulations also showed that the thermoelectric response of these detectors add linearly when connecting them in series.

Keywords: Infrared Detector, LWIR, Seebeck nanoantennas, Thermoelectric IR detectors

1. INTRODUCTION

Infrared imaging systems have become popular in high volume markets such as automotive, surveillance, industrial process control, night vision and medical imaging to name a few. Current technology is shifting to low cost and small size, weight and power (SWaP) infrared systems. Infrared imaging technology focuses on the detection of infrared radiation in the atmospheric windows in the mid infrared 3–5 μm (MWIR) and the long wave infrared 8–14 μm (LWIR). Most of the LWIR imaging systems rely on microbolometers for their Focal Plane Arrays, which have high time constants in the order of milliseconds and require a bias voltage to operate [1-2].

Seebeck nanoantennas convert electromagnetic energy into electrical energy through the thermoelectric effect. These devices are designed using either a material or geometrical asymmetry that facilitates thermal diffusion of electrons between a hot junction and a cold junction [3].

When coupled to antennas the electromagnetic energy induces a current in the antenna arms that heats the hot junction of the Seebeck nanoantenna, this hot junction is usually the point of contact between dissimilar materials and also the feed of the antenna. The choice of materials used impacts both the performance of the electromagnetic properties of the antenna and its thermoelectric properties.

These room temperature detectors can be designed for any IR band and their low thermal mass makes them faster than traditional bolometers. The IR-generated thermal current requires no bias power-supply. They are made of cheaper materials with simpler processing than traditional bolometers. Hence, they are ideal detectors for SWaP high-speed infrared imaging systems [4].

In this work the materials and fabrication process of the antenna and the thermoelectric connection of long wave bowtie Seebeck nanoantennas are optimized through numerical simulations in order to increase their responsivity. A fabrication process is discussed with initial results presented.

*javier.gonzalez@uaslp.mx

Image Sensing Technologies: Materials, Devices, Systems, and Applications VIII, edited by Nibir K. Dhar, Achyut K. Dutta, Sachidananda R. Babu, Proc. of SPIE Vol. 11723, 117230A

2. METHODS

The devices analyzed are Seebeck bowtie nanoantennas fabricated on a silicon dioxide substrate which provides thermal and electrical isolation (Fig. 1(a)). Three configurations are studied, a gap bowtie antenna made of gold with the thermoelectric elements connecting at the feed of the antenna (Fig. 1(a)), a free-standing Seebeck bowtie antenna (Fig. 1(b)), and a two-element array of free-standing bowtie antennas (Fig. 1(c)).

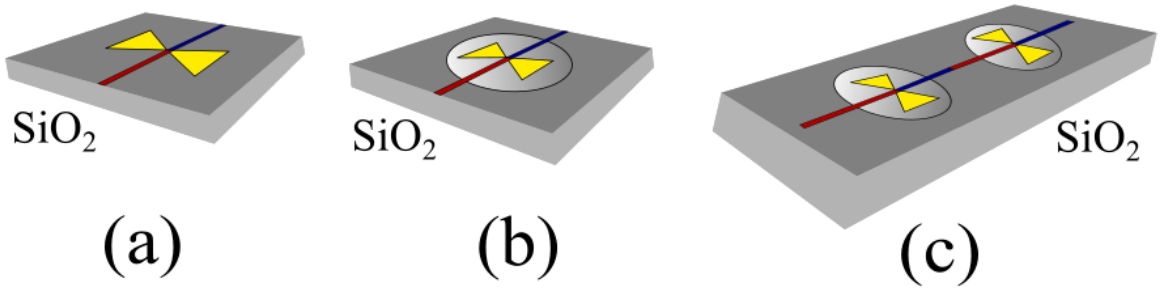

Figure 1. (a) Gap bowtie antenna made of gold with the thermoelectric elements connecting at the feed of the antenna, (b) free-standing Seebeck bowtie antenna, (c) two-element array of free-standing bowtie antennas.

The devices were evaluated numerically using the finite element method through the commercial software COMSOL Multiphysics, the simulation procedure consisted in launching a linearly polarized plane wave with an irradiance of 1000 W/m^2 over the surface of the Seebeck nanoantennas. The incident wave was polarized along the main axis of the bowtie antenna. A parametric simulation was performed by doing a frequency sweep of the incident plane wave from 3 to 60 THz. The induced current in the antenna, the increase in temperature due to Joule heating, as well as the output thermoelectric voltage were calculated coupling the electromagnetic, heat transfer and thermoelectric equations through a multi-physics simulation.

3. RESULTS

Finite element computer simulations of Seebeck bowtie nanoantennas were performed as a function of bowtie antenna length. Gold bowtie antennas on a SiO_2 substrate with Si-Bi_2Te_3 thermoelectric connections (Fig. 1(a)) were simulated for different bowtie lengths from 2 to 3.5 μm in 0.5 μm steps. Figure 2(a) shows the thermoelectric voltage that resulted from these simulations, from Fig. 2(a) can be seen that a bowtie length of 2 μm will have a full width half maximum (FWHM) detection range of 18-50 THz (6-16 μm) in the LWIR region of the electromagnetic spectrum. Figure 2(b) shows the comparison of two different thermoelectric connection lines and the same gold bowtie antenna, from Fig. 2(b) it can be seen that by using a Sb_2Te_3-Bi_2Te_3 thermoelectric connection line a 30% increase in voltage response is obtained with a more selective frequency response from 22-38 THz (8-13 μm) FWHM. This higher response is due to the lower thermal conductivity of Sb_2Te_3 compared to Si which increases the temperature at the feed of the bowtie nanoantenna [5].

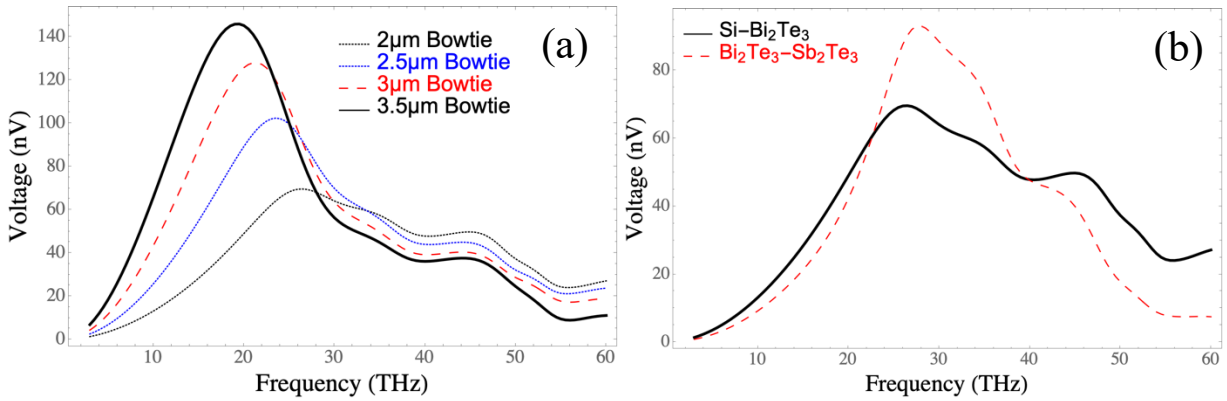

Figure 2. Thermoelectric voltage for (a) Gold bowtie antennas on a SiO_2 substrate with Si-Bi_2Te_3 thermoelectric connections and varying lengths from 2 to 3.5 μm in 0.5 μm steps, (b) comparison of two different thermoelectric connection lines and the same 2 μm long gold bowtie antenna.

The approximate collection area for metallic nanoantennas is equal to λ μm^2, where λ is the resonant wavelength of the nanoantenna in microns [1]. For nanoantennas tuned at 30 THz, like the ones shown in Fig. 2(b) the approximate collection area would be equal to 10 μm^2. Therefore the incident electromagnetic power collected by the nanoantenna would be 10 nW, giving a responsivity of 7 V/W and 9 V/W for 2 μm long bowtie antennas on a SiO_2 substrate with a Si-Bi_2Te_3 and Sb_2Te_3-Bi_2Te_3 thermoelectric lines respectively.

Additional simulations were performed on released devices where there is no contact with the substrate (Figs 1(b)-(c)), by isolating the devices from the substrate a greater thermal increase in the feed of the antenna will be achieved increasing its responsivity. These free standing structures can be fabricated by using SiO_2 as a sacrificial layer and generating an undercut below the gold bowtie antenna. The simulated free standing structures consisted of gold bowtie nanoantennas with a Sb_2Te_3-Bi_2Te_3 thermoelectric connection lines, a length study was performed since the electrical length changes depending on the index of refraction of the substrate. Figure 3(a) shows the response of the released structures with different bowtie lengths from 1.5 to 3 μm in 0.5 μm steps. Figure 3(a) indicates that a 3 μm long gold bowtie antenna will detect a FWHM range of frequencies from 22-38 THz (8-13 μm) with a maximum voltage of 2.4 μV at 28 THz, which gives an approximate 25× increase in response compared to a similar antenna on a SiO_2 substrate. Figure 3(b) shows the voltage response comparison of a single bowtie Seebeck nanoantenna and a 2-array of bowtie nanoantennas connected in series. From Fig. 3(b) it can be seen that the voltage response adds linearly with the number of nanoantennas in the array. The voltage responsivity for these released devices is 240 V/W.

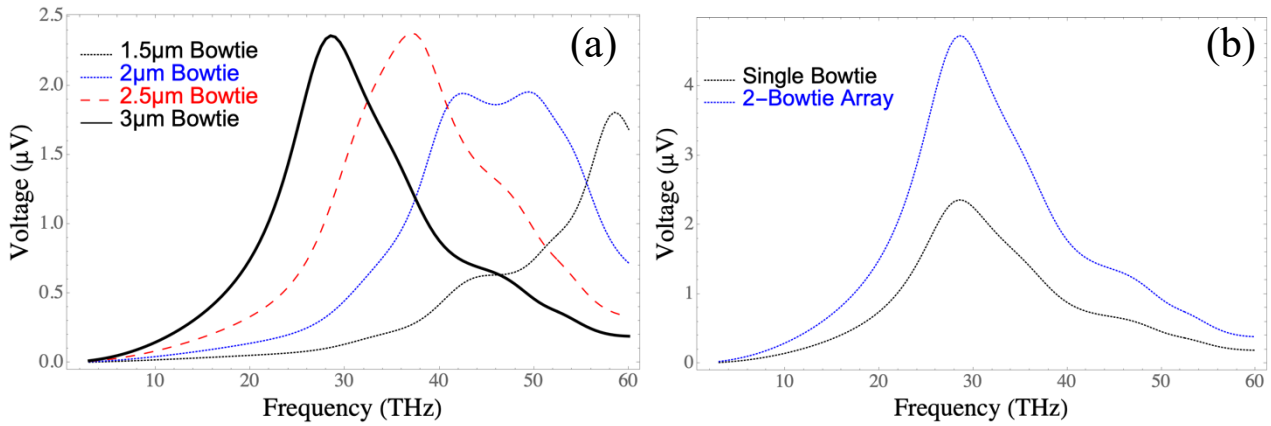

Figure 3. (a) Response of the released gold bowtie antenna structures with different bowtie lengths from 1.5 to 3 μm in 0.5 μm steps and Sb_2Te_3-Bi_2Te_3 thermoelectric connection lines. (b) Voltage response comparison of a single bowtie Seebeck nanoantenna and a 2-array of bowtie nanoantennas connected in series.

Figure 4 shows the electric potential due to the thermoelectric effect on two serially connected gold bowtie antennas with Sb2Te3-Bi2Te3 thermoelectric connection lines (Fig 1(c)).

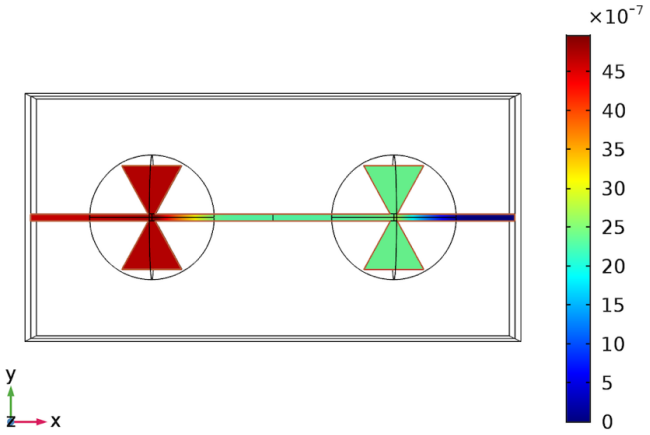

Figure 4. electric potential due to the thermoelectric effect on two serially connected gold bowtie antennas with Sb_2Te_3-Bi_2Te_3 thermoelectric connection lines.

Figure 5 presents an image of a fabricated Seebeck nanoantenna. The bowtie is gold, the linear traces are Bi_2Te_3 and Sb_2Te_3, with their junction at the center of the bowtie. A simple three-step process flow is designed for fabrication of the proof-of-concept devices disclosed in this paper. The devices are fabricated on a glass or quartz wafer in order to minimize the heat conduction through the substrate and to improve the sensitivity of the device. The three different thin-films that the device is comprised of: Bismuth Telluride (Bi_2Te_3), Antimony Telluride (Sb_2Te_3), and Gold are deposited in a sequence using RF magnetron sputtering (for Bi_2Te_3 and Sb_2Te_3) and e-beam evaporation (for gold). All three films are patterned using lift-off and a thin layer of Chromium is used as adhesion layer to promote the adhesion of the gold layer. A resistive heater is also formed from the Cr/Gold layer next to the junction. This heater will be used to characterize the thermoelectric response of the junction before the sensors are utilized for THz radiation detection. Through this technique we have already confirmed that the Seebeck coefficients of the sputtered Bi_2Te_3 and Sb_2Te_3 films are negative and positive respectively indicating that the films are n-type and p-type as expected [6].

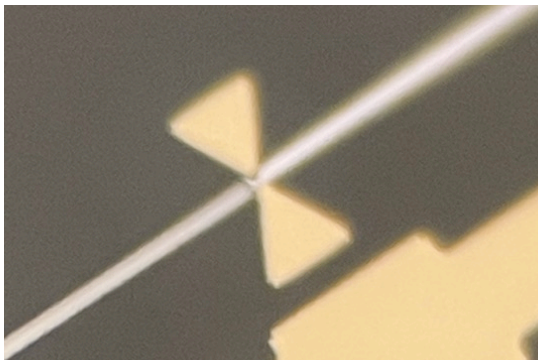

Figure 5. Optical microscope image of fabricated bowtie Seebeck nanoantenna

4. CONCLUSIONS

Finite element computer simulations of Seebeck bowtie nanoantennas were performed in the long wave infrared by using different thermoelectric connection lines and changing the thermal conduction through the substrate. Different thermal conduction through the substrate was achieved by simulating these detectors on a SiO_2 substrate and as free-standing structures on air. Results showed that gold bowtie nanoantennas with thermoelectric connections made of Bi_3Te_2 and Sb_3Te_2 had responsivity values of 9 V/W on a SiO_2 substrate and 240 V/W as free-standing structures. Computer simulations also showed that the thermoelectric response of these type of antennas add linearly when building them into arrays. These results indicate that Seebeck nanoantennas can be used as low cost and small size, weight and power (SWaP) long wave infrared detectors.

ACKNOWLEDGMENTS

FJG Acknowledges Financial Support From Fondo Sectorial Conacyt-Sener- Sustentabilidad Energética Through Grant 207450, “Centro Mexicano De Innovación En Energía Solar (CEMIE- SOL)”, Within Strategic Project No. P105.

REFERENCES

[1] González, F. J. & Boreman, G. D. Comparison of dipole, bowtie, spiral and log-periodic IR antennas. Infrared Phys. Technol.46, 418–428, (2005).
[2] Brhayllan Mora-Ventura, Ramón Díaz de León, Guillermo García-Torales, Jorge L. Flores, Javier Alda, Francisco J. González, “Responsivity and resonant properties of dipole, bowtie, and spiral Seebeck nanoantennas,” J. Photon. Energy 6(2), 024501 (2016).
[3] González, F., Dhakal, N., Boykin, T., Méndez-Lozoya, J., & Peale, R. (2020). Infrared pixel based on Seebeck nanoantennas. MRS Advances, 5(35-36), 1837-1842.

[4] Szakmany, G.P., Bernstein, G.H., Kinzel, E.C. *et al.* Nanoantenna-based ultrafast thermoelectric long-wave infrared detectors. *Sci Rep* **10,** 13429 (2020).
[5] G. J. Snyder and A. H. Snyder, "Figure of merit ZT of a thermoelectric device defined from materials properties," Energy Environ. Sci., 10, pp. 2280-2283, (2017).
[6] M, Mizue, M. Mikami, and K. Ozaki. "P-Type Sb_2Te_3 and n-type Bi_2Te_3 films for thermoelectric modules deposited by thermally assisted sputtering method." *Japanese Journal of Applied Physics* 52, no. 6S (2013): 06GL07.